

# Interval uncertainty propagation by a parallel Bayesian global optimization method

Chao Dang<sup>a</sup>, Pengfei Wei<sup>b,\*</sup>, Matthias G.R. Faes<sup>c</sup>, Marcos A. Valdebenito<sup>d</sup>, Michael Beer<sup>a,e,f</sup>

<sup>a</sup>*Institute for Risk and Reliability, Leibniz University Hannover, Callinstr. 34, Hannover 30167, Germany*

<sup>b</sup>*School of Mechanics, Civil Engineering and Architecture, Northwestern Polytechnical University, Xi'an 710072, PR China*

<sup>c</sup>*Chair for Reliability Engineering, TU Dortmund University, Leonhard-Euler-Str. 5, Dortmund 44227, Germany*

<sup>d</sup>*Faculty of Engineering and Sciences, Universidad Adolfo Ibáñez, Av. Padre Hurtado 750, 2562340 Viña del Mar, Chile*

<sup>e</sup>*Institute for Risk and Uncertainty, University of Liverpool, Liverpool L69 7ZF, United Kingdom*

<sup>f</sup>*International Joint Research Center for Resilient Infrastructure & International Joint Research Center for Engineering Reliability and Stochastic Mechanics, Tongji University, Shanghai 200092, PR China*

---

## Abstract

This paper is concerned with approximating the scalar response of a complex computational model subjected to multiple input interval variables. Such task is formulated as finding both the global minimum and maximum of a computationally expensive black-box function over a prescribed hyper-rectangle. On this basis, a novel non-intrusive method, called ‘triple-engine parallel Bayesian global optimization’, is proposed. The method begins by assuming a Gaussian process prior (which can also be interpreted as a surrogate model) over the response function. The main contribution lies in developing a novel infill sampling criterion, i.e., triple-engine pseudo expected improvement strategy, to identify multiple promising points for minimization and/or maximization based on the past observations at each iteration. By doing so, these identified points can be evaluated on the real response function in parallel. Besides, another potential benefit is that both the lower and upper bounds of the model response can be obtained with a single run of the developed method. Four numerical examples with varying complexity are investigated to demonstrate the proposed method against some existing techniques, and results indicate that significant computational savings can be achieved by making full use of prior knowledge and parallel computing.

*Keywords:* Interval uncertainty propagation, Bayesian global optimization, Gaussian process, Infill sampling criterion, Parallel computing

## Abbreviations

3-D	three-dimensional	PEI	pseudo expected improvement
BGO	Bayesian global optimization	PEI-MAX	pseudo expected improvement for maximum
EI	expected improvement	PEI-MIN	pseudo expected improvement for minimum
EI-MAX	expected improvement for maximum	PEI-MIN-MAX	pseudo expected improvement for minimum and maximum
EI-MIN	expected improvement for minimum	T-PBGO	triple-engine parallel Bayesian global optimization
GP	Gaussian process	T-PEI	triple-engine pseudo expected improvement
I-MLQMC	interval multilevel quasi-Monte Carlo	TLBO	teaching-learning-based optimization
LHS	Latin hypercube sampling		
N-PBGO	non-parallel Bayesian global optimization		
NLML	negative log marginal likelihood		
PBGO	parallel Bayesian global optimization		

## 29 1. Introduction

30 Along with the rapid development of computation techniques, deterministic numerical analysis has made  
31 great progress in various fields over the past several decades [1]. In this context, all parameters of a  
32 computational model designed to describe underlying structures or systems are typically treated as precise  
33 (crisp) numbers. This kind of numerical analysis, however, is essentially not suitable for situations where  
34 non-determinism has to be properly considered, which is the common case for a broad range of modern  
35 science and engineering disciplines. A typical example of such situations is the design and analysis of

---

\*Corresponding author

*Email addresses:* [chao.dang@irz.uni-hannover.de](mailto:chao.dang@irz.uni-hannover.de) (Chao Dang), [pengfeiwei@nwpu.edu.cn](mailto:pengfeiwei@nwpu.edu.cn) (Pengfei Wei),  
[matthias.faes@tu-dortmund.de](mailto:matthias.faes@tu-dortmund.de) (Matthias G.R. Faes), [marcos.valdebenito@uai.cl](mailto:marcos.valdebenito@uai.cl) (Marcos A. Valdebenito),  
[beer@irz.uni-hannover.de](mailto:beer@irz.uni-hannover.de) (Michael Beer)

36 engineering systems at an early stage where many aspects could be only imprecisely known. Alternatively,  
37 non-deterministic numerical analysis is emerging as an exciting research frontier with new opportunities  
38 and also challenges. **Such opportunities and challenges arise throughout the whole analysis, e.g.,**  
39 **non-determinism characterization on the input side and response uncertainty quantification**  
40 **on the output side.**

41 In general, three types of approaches are available for modelling non-determinism: probabilistic approach,  
42 imprecise probabilistic approach and non-probabilistic approach [2]. On the basis of classical probability  
43 theory and statistical techniques, the probabilistic approach is most widely used. Herein, an uncertain  
44 parameter is modelled as a random variable with a precisely known probability distribution. Thus, it is  
45 often challenging to apply the probabilistic approach in reality since a large amount of high-quality data is  
46 required to infer an accurate probability distribution. Against this background, by generalizing traditional  
47 probability and statistics concepts, the imprecise probabilistic approach has evolved as a powerful and elegant  
48 framework for quantifying uncertainty from incomplete information [3, 4]. Within this approach, one needs  
49 to assign a pair of lower and upper probabilities to an event, rather than a single probability. On the other  
50 hand, the non-probabilistic approach, such as interval models and fuzzy sets [5], is also gaining increasing  
51 interest for non-determinism modelling, **especially when the available information is limited.** With  
52 the interval concept, a non-deterministic parameter is treated as an interval variable specified by a pair  
53 of numbers, i.e., the lower and upper bounds, and potentially a function modelling the auto-dependencies  
54 among multiple interval parameters [6]. Thus, instead of a full probability distribution the analyst only needs  
55 to determine the bounds and auto-dependency functions, which can be easily and objectively acquired from  
56 a small number of samples. The present study limits its scope to interval uncertainty.

57 There have been plenty of methods developed to propagate interval uncertainty via a computational  
58 model, which can be roughly classified into four kinds. The first kind of methods is based on using the  
59 interval arithmetic of Moore, e.g., refer to [7]. Despite its efficiency, the interval calculus cannot trace  
60 parameter dependency by definition (the so-called dependency problem), which therefore can lead to a  
61 severe overestimation of the size of a response interval. **Recent developments are focused on limiting**

62 the overestimation by, e.g., accounting for dependency among interval variables [8–12] or  
63 using interval fields [13, 14], parameterizing intervals via trigonometric functions [15, 16]  
64 and representing intervals by affine arithmetic [17, 18], etc. Although these methods are able to  
65 provide sharp bounds within reasonable computational cost, their applicability is still limited due to the  
66 intrusive nature of interval arithmetic. The approximate analytical methods that rely on constructing a  
67 simplified approximation of true response function falls in the second group. Typical examples of such  
68 methods include, Taylor series expansion methods [19–23] and Chebyshev series expansion methods [24, 25],  
69 which are intrusive and non-intrusive, respectively. However, these Taylor methods tend to lose accuracy  
70 when the considered problem involves large uncertainty (i.e., the widths of interval variables being large)  
71 and/or highly nonlinear behavior. For these Chebyshev methods, the required number of response function  
72 evaluations grows exponentially with the number of dimensions. As for the third type, the vertex method  
73 [26, 27] and interval multilevel quasi-Monte Carlo (I-MLQMC) [28, 29] are non-intrusive and can produce  
74 accurate response bounds under certain conditions. The classical vertex method is exact on the premise  
75 that the response function is monotonic with respect to  $d$  interval parameters, while at the cost of  $2^d$  model  
76 evaluations. More strictly, the I-MLQMC method requires a linearity assumption on the response function.  
77 As such, these two methods suffer from non-linearity and/or dimensionality.

78 In the last group, global optimization methods are naturally applicable to the topic of interval numerical  
79 analysis. In this context, several studies have been conducted by directly using, e.g., genetic algorithm  
80 [30, 31]. Generally, global optimization algorithms require a large number of model evaluations to find the  
81 minimum/maximum, and hence can be computationally demanding especially when each such evaluation  
82 is expensive. To alleviate the computation burden, a cheap-to-evaluate surrogate model can be adopted to  
83 substitute the original computational model based on some observations. Along this line, Kriging-assisted  
84 global optimization (formally called Bayesian global optimization (BGO)) algorithms are attracting increas-  
85 ing attention due to their high efficiency for optimizing expensive black-box functions. A typical BGO  
86 method starts by building an initial Kriging model for the objective function based on a small number of  
87 observations, and then refines the initial model by sequentially selecting more updating points according to a

88 infill sampling criterion [32]. Existing studies then focus more on developing efficient infill sampling criteria  
89 so as to reduce the total number of function evaluations. On this aspect, representative works in the context  
90 of interval uncertainty propagation include the maximum improvement criterion [33], expected improvement  
91 criterion [34, 35] and a comparison study of several criteria [36]. **It is shown that these methods exhibit  
92 encouraging features regarding the computational efficiency and accuracy for computationally  
93 expensive black-box problems over other existing methods. Despite these advantages, one  
94 of the major limitations of the existing BGO methods is that they are sequential in nature  
95 and hence unsuitable for parallelization, or at least high-level parallelization, hindering the  
96 potential benefits from parallel distributed processing.**

97 In this paper, a parallel Bayesian global optimization (PBGO) method is proposed for estimating the  
98 response bounds of a computational model in the presence of interval variables. Our main objective is to  
99 further reduce the computational time of existing BGO methods by making use of parallelism. For this  
100 purpose, a novel infill sampling criterion is developed to select multiple points at each iteration, and hence  
101 corresponding model evaluations can be distributed on multiple processing cores simultaneously. **Such  
102 parallelisation is relevant when the model at hand is computationally intensive and parallel  
103 computing facilities are available. Besides, in contrast to the traditional way of searching the  
104 lower and upper bounds of a scalar response quantity via two separate optimization problems,  
105 we consider it only as one problem.** Following the developed scheme, the lower and upper bounds can  
106 be obtained simultaneously with a single run. Last but not least, a Matlab implementation of the developed  
107 algorithm is also readily available to the public <sup>1</sup>.

108 The remainder of the paper is organized as follows. Section 2 describes the interval analysis problem to  
109 be solved in this study. The proposed PBGO method is introduced in Section 3, with its relationship to other  
110 PBGO methods also being discussed. Four numerical examples are studied in Section 4 to demonstrate the  
111 performance of the developed method. In Section 5, some concluding remarks and perspectives are given to  
112 end the paper

---

<sup>1</sup>to be released upon acceptance of the paper

113 **2. Problem formulation**

114 Let us consider a computational model represented by a deterministic, continuous, and real-valued func-  
 115 tion  $y = g(\mathbf{x}) : \mathbb{R}^d \rightarrow \mathbb{R}$ . Here the model response  $y$  is a scalar quantity of interest, the  $g$ -function is  
 116 assumed to be an expensive-to-evaluate black box, and the model input vector  $\mathbf{x}$  consists of  $d$  variables, i.e.,  
 117  $\mathbf{x} = [x_1, x_2, \dots, x_d]$ .

118 Under the assumption that available information on the model inputs is poor or incomplete, we proceed  
 119 to treat them with interval models. **For identifying intervals from real observations, one can refer**  
 120 **to, e.g., [37, 38].** An interval vector  $\mathbf{x}^I = [x_1^I, x_2^I, \dots, x_d^I] \in \mathbb{IR}^d$  can be defined as:

$$\mathbf{x}^I = [\underline{\mathbf{x}}, \bar{\mathbf{x}}] = \{\mathbf{x} \in \mathbb{R}^d | \underline{\mathbf{x}} \leq \mathbf{x} \leq \bar{\mathbf{x}}\}, \quad (1)$$

and its component  $x_i^I$  satisfies

$$x_i^I = [\underline{x}_i, \bar{x}_i] = \{x \in \mathbb{R} | \underline{x}_i \leq x \leq \bar{x}_i\}, i = 1, 2, \dots, d,$$

where  $\underline{\mathbf{x}} = [\underline{x}_1, \underline{x}_2, \dots, \underline{x}_d]$  and  $\bar{\mathbf{x}} = [\bar{x}_1, \bar{x}_2, \dots, \bar{x}_d]$  represent the lower and upper bounds of  $\mathbf{x}^I$ , respectively.

Further, the midpoint  $\mathbf{x}^C$  and radius  $\mathbf{x}^R$  of  $\mathbf{x}^I$  can be defined as:

$$\mathbf{x}^C = \frac{\underline{\mathbf{x}} + \bar{\mathbf{x}}}{2},$$

$$\mathbf{x}^R = \frac{\bar{\mathbf{x}} - \underline{\mathbf{x}}}{2}.$$

It follows that the interval vector defined in Eq. (1) can also be rewritten in terms of  $\mathbf{x}^C$  and  $\mathbf{x}^R$  as:

$$\mathbf{x}^I = \mathbf{x}^C + \delta\mathbf{x},$$

121 where  $\delta\mathbf{x} \in [-1, 1]\mathbf{x}^R$ . **For convenience, the interval variables are assumed to be independent.**  
 122 **In fact, for dependent interval variables one can transform them into independent ones by**  
 123 **applying a suitable transformation, e.g., [39].**

124 With the interval vector  $\mathbf{x}^I$  as input, the  $g$ -function will also give rise to a interval output  $y^I$  in our  
 125 context, i.e.,  $y^I = \{y \in \mathbb{R} | y = g(\mathbf{x}), \mathbf{x} \in \mathbf{x}^I\}$ . The resulting interval can be fully characterized by its lower  
 126 and upper bounds, which correspond to the worst or best case of  $y^I$  that we might be interested in. Therefore,

127 the main objective is to determine the lower and upper bounds of  $y^I$ , which are naturally defined as the  
 128 solutions of the following two optimization problems:

$$\underline{y} = \min_{\mathbf{x} \in \mathbf{x}^I} \{y | y = g(\mathbf{x})\}, \quad (2)$$

129

$$\bar{y} = \max_{\mathbf{x} \in \mathbf{x}^I} \{y | y = g(\mathbf{x})\}, \quad (3)$$

130 where  $\underline{y}$  and  $\bar{y}$  can be interpreted as the global minimum and maximum of  $y = g(\mathbf{x})$  subject to  $\mathbf{x} \in \mathbf{x}^I$ ,  
 131 respectively.

132 Although their definitions are rather simple, the analytical solutions to  $\underline{y}$  and  $\bar{y}$  are unavailable for a  
 133 general black-box problem. Thus, numerical approximation techniques are necessary and useful tools for  
 134 practical applications. Existing numerical methods, however, still suffer from their respective limitations  
 135 as discussed in the introduction section. This motivates us to develop a PBGO method for propagating  
 136 interval uncertainty in the following section.

### 137 3. Triple-engine parallel Bayesian global optimization

138 In this section, the propagation of interval uncertainty via an expensive black-box computational model is  
 139 treated by a kind of Bayesian numerical method, i.e., the so-called Bayesian global optimization (BGO) [32].  
 140 Specifically, an efficient method, termed ‘‘Triple-engine parallel Bayesian global optimization’’ (T-PBGO),  
 141 is proposed to approximate the lower and upper bounds of the model output  $y^I$  (defined in Eqs. (2) and  
 142 (3)) when the model input is characterized by a interval vector  $\mathbf{x}^I$  (defined in Eq. (1)). The proposed  
 143 method makes use of the Gaussian process model and a newly developed infill sampling criterion, as will be  
 144 introduced in what follows. For notational simplicity, the superscripts of  $\mathbf{x}^I$  and  $y^I$  are omitted when there  
 145 is no confusion.

#### 146 3.1. Gaussian process model

Under the black-box assumption, no additional knowledge on the inner structure of the  $g$ -function is available and the only possibility for us is to evaluate it at some points. That is, we know nothing about the behavior of the  $g$ -function (e.g., concavity and linearity) before seeing any observations, let along its

minimum and maximum. The lack of knowledge on  $g(\cdot)$  is referred to as a kind of epistemic uncertainty simply because it is numerically unknown until we actually evaluate it, and hence reduceable. Following a Bayesian approach, our prior beliefs on the  $g$ -function can be modeled by assigning a Bayesian prior distribution. In this study, we adopt a Gaussian process (GP) prior over  $g$ . In the following, we only give a brief introduction to the GP model, and for further details the reader can refer to [40]. The GP prior assumes that the  $g$ -function is a realization of a GP indexed by  $\mathbf{x}$ . To formalize this, we write the GP prior as:

$$\hat{g}_0(\mathbf{x}) \sim \mathcal{GP}(m_0(\mathbf{x}), k_0(\mathbf{x}, \mathbf{x}')) = m_0(\mathbf{x}) + Z(\mathbf{x}),$$

where  $\hat{g}_0$  denotes the prior distribution of  $g$ ;  $m_0(\mathbf{x})$  is the mean function of the GP prior;  $Z(\mathbf{x})$  is a stationary GP with zero-mean and covariance function  $k_0(\mathbf{x}, \mathbf{x}')$ . The GP prior is completely characterized by its prior mean function  $m_0(\mathbf{x})$  and covariance function  $k_0(\mathbf{x}, \mathbf{x}')$ . The prior mean function reflects the general trend of the GP model, while the prior covariance function encodes the key features of the  $g$ -function, e.g., stationarity, isotropy, smoothness and periodicity. **There are many kinds of specific functional forms available in literature for the prior mean and covariance functions [40].** In this paper, without loss of generality, the prior mean function is assumed to be a constant (i.e.,  $m_0(\mathbf{x}) = \beta$ ) and the prior covariance function is of squared exponential form expressed as:

$$k_0(\mathbf{x}, \mathbf{x}') = \sigma_g^2 \exp \left[ -\frac{1}{2} (\mathbf{x} - \mathbf{x}')^\top \boldsymbol{\Sigma}^{-1} (\mathbf{x} - \mathbf{x}') \right],$$

147 where  $\sigma_g^2$  is the overall variance with  $\sigma_g > 0$ ;  $\boldsymbol{\Sigma} = \text{diag}(l_1^2, l_2^2, \dots, l_d^2)$  with  $l_i > 0$  being the characteristic  
148 length-scale in  $i$ -th dimension; and  $\text{diag}(\cdot)$  denotes a diagonal matrix whose entries are equal to the argument  
149 values. The  $d + 2$  free parameters  $\beta$ ,  $\sigma_g^2$  and  $\{l_i\}_{i=1}^d$  are referred to hyper-parameters whose values need to  
150 be determined, denoted by  $\boldsymbol{\theta} = \{\beta, \sigma_g^2, l_1, l_2, \dots, l_d\}$ .

151 Now assume that we have evaluated the  $g$ -function at several (e.g.,  $n \in \mathbb{Z}^+$ ) points. We aggregate the  
152 sampled points in a  $n \times d$  matrix  $\mathbf{X}$  with its  $j$ -th row being the  $j$ -th point  $\mathbf{x}^{(j)}$ , and the corresponding  
153  $g$ -function values in a  $n \times 1$  vector  $\mathbf{y}$  with its  $j$ -th element being  $y^{(j)}$ , where  $y^{(j)} = g(\mathbf{x}^{(j)})$ . The set of



154 hyper-parameters can then be estimated by minimizing the negative log marginal likelihood (NLML) [40]:

$$\hat{\boldsymbol{\theta}} = \arg \min_{\boldsymbol{\theta}} (-\log [p(\mathbf{y}|\mathbf{X}, \boldsymbol{\theta})]), \quad (4)$$

155 with

$$-\log [p(\mathbf{y}|\mathbf{X}, \boldsymbol{\theta})] = \frac{1}{2}(\mathbf{y} - \beta)^\top \mathbf{K}_0^{-1}(\mathbf{y} - \beta) + \frac{1}{2} \log [|\mathbf{K}_0|] + \frac{n}{2} \log [2\pi], \quad (5)$$

156 where  $\mathbf{K}_0$  is a  $n \times n$  covariance matrix with its  $(i, j)$ -th entry being  $[\mathbf{K}_0]_{ij} = k_0(\mathbf{x}^{(i)}, \mathbf{x}^{(j)})$ . Eq. (4) can be  
 157 solved by gradient-based optimization schemes since the derivatives of NLML in Eq. (5) with respect to  $\boldsymbol{\theta}$   
 158 are analytically tractable.

Conditioning on the observations  $(\mathbf{X}, \mathbf{y})$  and GP prior will give rise to a posterior distribution  $\hat{g}_n$  of  $g$ . This distribution still follows a GP  $\hat{g}_n(\mathbf{x}) \sim \mathcal{GP}(m_n(\mathbf{x}), k_n(\mathbf{x}, \mathbf{x}'))$ , with the posterior mean and covariance functions as follows:

$$m_n(\mathbf{x}) = m_0(\mathbf{x}) + \mathbf{k}_0(\mathbf{x}, \mathbf{X})\mathbf{K}_0^{-1}(\mathbf{y} - \mathbf{m}_0(\mathbf{X})),$$

$$k_n(\mathbf{x}, \mathbf{x}') = k_0(\mathbf{x}, \mathbf{x}') - \mathbf{k}_0(\mathbf{x}, \mathbf{X})\mathbf{K}_0^{-1}\mathbf{k}_0(\mathbf{x}', \mathbf{X})^\top,$$

159 where  $\mathbf{k}_0(\mathbf{x}, \mathbf{X})$  is a  $1 \times n$  covariance vector between  $\mathbf{x}$  and  $\mathbf{X}$ , whose  $j$ -th element is  $k_0(\mathbf{x}, \mathbf{x}^{(j)})$ ;  $\mathbf{k}_0(\mathbf{x}', \mathbf{X})$  is  
 160 similarly defined;  $\mathbf{m}_0(\mathbf{X})$  is a  $n \times 1$  mean vector, whose  $j$ -th element is  $m_0(\mathbf{x}^{(j)})$ . It is seen that via a Bayesian  
 161 treatment a full predictive distribution  $\hat{g}(\mathbf{x}) \sim \mathcal{N}(m_n(\mathbf{x}), \sigma_n^2(\mathbf{x}))$  is now available, where the posterior mean  
 162 function  $m_n(\mathbf{x})$  can be used as a predictor, while the posterior variance function  $\sigma_n^2(\mathbf{x}) = k_n(\mathbf{x}, \mathbf{x})$  can  
 163 measure the prediction uncertainty.

### 164 3.2. Proposed triple-engine pseudo expected improvement criterion

165 In order to make inference about the minimum and maximum of the  $g$ -function using as few function  
 166 evaluations as possible, our main concern is to design an efficient infill sampling criterion that can effectively  
 167 suggest future evaluation points based on the posterior GP (implicitly the past observations). In particular,  
 168 we seek to identify a batch of **informative and diverse** points at each iteration. Hence, multiple evaluations  
 169 of the  $g$ -function can be distributed on several cores simultaneously so as to reduce the overall wall-clock  
 170 time. For convenience of illustration, we assume that the number of points we would like to select at

171 each iteration is a even number  $q$  in sequel, though it should not to be. Our purposes are achieved by  
 172 generalizing the pseudo expected improvement (PEI) criterion [41], which has been recently developed in  
 173 the field of global optimization, to an enhanced version, termed ‘triple-engine pseudo expected improvement’  
 174 (T-PEI) criterion. **The T-PEI criterion actually involves a set of three infill sampling criteria**  
 175 **that we call them ‘engines’, as discussed below.**

### 176 3.2.1. Engine 1: PEI for minimum

177 The first engine is the PEI criterion originally developed in [41] for global minimization  
 178 problems (denoted by PEI-MIN for convenience). In the present study, this criterion will  
 179 be directly used to select  $q$  promising points for the propose of minimizing the  $g$ -function  
 180 wherever applicable.

181 Let  $y_{\min} = \min_{1 \leq j \leq n} y^{(j)}$  indicate the minimum value of  $y$  observed so far. The improvement  
 182 at point  $\mathbf{x}$  over the current best solution  $y_{\min}$  can be defined as [32]:

$$I_{\min}(\mathbf{x}) = \max(y_{\min} - \hat{g}_n(\mathbf{x}), 0) = \begin{cases} y_{\min} - \hat{g}_n(\mathbf{x}), & \text{if } \hat{g}_n(\mathbf{x}) < y_{\min} \\ 0, & \text{otherwise} \end{cases}, \quad (6)$$

183 which is a random variable at site  $\mathbf{x}$ . The so-called expected improvement (EI) over the current  
 184 minimum  $y_{\min}$  consists of taking expectation of  $I_{\min}(\mathbf{x})$ , and can be derived in a closed-form  
 185 expression as [32]:

$$EI_{\min}(\mathbf{x}) = \mathbb{E}[I_{\min}(\mathbf{x})] = (y_{\min} - m_n(\mathbf{x}))\Phi\left(\frac{y_{\min} - m_n(\mathbf{x})}{\sigma_n(\mathbf{x})}\right) + \sigma_n(\mathbf{x})\phi\left(\frac{y_{\min} - m_n(\mathbf{x})}{\sigma_n(\mathbf{x})}\right), \quad (7)$$

186 where  $\phi(\cdot)$  and  $\Phi(\cdot)$  are the probability density function and cumulative distribution function  
 187 of the standard normal variable, respectively. The next best point be acquired within the  
 188 minimization process can be selected by maximizing  $EI_{\min}(\mathbf{x})$ , i.e.,

$$\mathbf{x}_{\min}^{(n+1)} = \arg \max_{\mathbf{x} \in \mathbf{x}^I} EI_{\min}(\mathbf{x}). \quad (8)$$

189 This criterion is referred to as EI-MIN for the sake of convenience. Note that the first term of  
 190  $EI_{\min}(\mathbf{x})$  (see Eq. (7)) prefers the point whose prediction  $m_n(\mathbf{x})$  is small, whereas the second

191 term prefers the point whose variance  $\sigma_n^2(x)$  is large. Thus, the EI-MIN criterion gives an  
 192 elegant balance between exploitation (i.e., local search) and exploration (i.e., global search).  
 193 Despite this, the EI-MIN criterion can only produce one single point at each iteration, and  
 194 hence not suitable for parallelization.

195 To overcome the limitation, the basic idea of the PEI-MIN criterion is to modify the initial  
 196 EI function (Eq. (7)) sequentially, by multiplying it by an influence function. That is, the first  
 197 updating point  $\mathbf{x}_{\min}^{(n+1)}$  is still generated by using the initial EI-MIN criterion (Eq. (8)). Then,  
 198 the second one  $\mathbf{x}_{\min}^{(n+2)}$  can be identified by maximizing a modified EI function that considers  
 199 the possible impact of the first updated point bringing to the EI function. In such a sequential  
 200 way, a desired number of points can be obtained at each iteration without evaluating the  $g$ -  
 201 function at any newly selected points. Thus, a good influence function should capture the real  
 202 influence of the newly identified points on the initial EI function as much as possible, while  
 203 remaining computationally tractable. The influence function proposed in [41] is motivated by  
 204 the fact that the EI function (Eq. (7)) is zero at the sampled points, and positive in between.  
 205 After  $q-1$  points have been identified, the synthesized influence function for the  $q$ -th point is  
 206 formulated as [41]:

$$\begin{aligned}
 IF(\mathbf{x}; \mathbf{x}_{\min}^{(n+1)}, \mathbf{x}_{\min}^{(n+2)}, \dots, \mathbf{x}_{\min}^{(n+q-1)}) &= \prod_{j=1}^{q-1} \left[ 1 - \rho \left( \mathbf{x}, \mathbf{x}_{\min}^{(n+j)} \right) \right] \\
 &= \prod_{j=1}^{q-1} \left[ 1 - \exp \left[ -\frac{1}{2} \left( \mathbf{x} - \mathbf{x}_{\min}^{(n+j)} \right)^{\top} \Sigma^{-1} \left( \mathbf{x} - \mathbf{x}_{\min}^{(n+j)} \right) \right] \right], \tag{9}
 \end{aligned}$$

207 where  $\rho \left( \mathbf{x}, \mathbf{x}_{\min}^{(n+j)} \right)$  is the correlation function between two points  $\mathbf{x}$  and  $\mathbf{x}_{\min}^{(n+j)}$ . It should be  
 208 noted that the influence function is zero at the  $q-1$  newly selected points  $\mathbf{x}_{\min}^{(n+1)}, \mathbf{x}_{\min}^{(n+2)}, \dots, \mathbf{x}_{\min}^{(n+q-1)}$ ,  
 209 and approaches to one when far away from these points. The PEI function for the  $q$ -th point  
 210 can be defined as [41]:

$$PEI_{\min}(\mathbf{x}; \mathbf{x}_{\min}^{(n+1)}, \mathbf{x}_{\min}^{(n+2)}, \dots, \mathbf{x}_{\min}^{(n+q-1)}) = EI_{\min}(\mathbf{x}) \times IF(\mathbf{x}; \mathbf{x}_{\min}^{(n+1)}, \mathbf{x}_{\min}^{(n+2)}, \dots, \mathbf{x}_{\min}^{(n+q-1)}). \tag{10}$$

The  $PEI_{\min}$  function can be interpreted as an approximation of the ‘real’  $EI_{\min}$  function because it is constructed without evaluating the  $g$ -function at these  $q-1$  points and updating

the GP model (i.e., re-evaluating the hyper-parameters). Besides, it reduces to the standard  $EI_{\min}$  function when  $q = 1$ , and hence the standard  $EI_{\min}$  function can be seen as a special case of the PEI function. The  $q$ -th point can be selected by maximizing the  $PEI_{\min}$  function such that:

$$\mathbf{x}_{\min}^{(n+q)} = \arg \max_{\mathbf{x} \in \mathbf{x}^I} PEI_{\min}(\mathbf{x}; \mathbf{x}_{\min}^{(n+1)}, \mathbf{x}_{\min}^{(n+2)}, \dots, \mathbf{x}_{\min}^{(n+q-1)}).$$

211 3.2.2. Engine 2: PEI for maximum

212 Inspired by the PEI-MIN criterion, we can also define a similar criterion to select  $q$  promis-  
 213 ing points for maximizing the  $g$ -function if needed. The resulting criterion is called PEI-MAX,  
 214 which is regarded as the second engine.

215 Let  $y_{\max} = \max_{1 \leq j \leq n} y^{(j)}$  denote the maximum value of  $y$  among the past  $n$  observations. In  
 216 analogy to Eq. (6), the improvement at point  $\mathbf{x}$  beyond the current best solution  $y_{\max}$  can be  
 217 defined as:

$$I_{\max}(\mathbf{x}) = \max(\hat{g}_n(\mathbf{x}) - y_{\max}, 0) = \begin{cases} \hat{g}_n(\mathbf{x}) - y_{\max}, & \text{if } \hat{g}_n(\mathbf{x}) > y_{\max} \\ 0, & \text{otherwise} \end{cases}. \quad (11)$$

218 The EI for the maximum is analytically derived in closed form as follows:

$$EI_{\max}(\mathbf{x}) = \mathbb{E}[I_{\max}(\mathbf{x})] = (m_n(\mathbf{x}) - y_{\max})\Phi\left(\frac{m_n(\mathbf{x}) - y_{\max}}{\sigma_n(\mathbf{x})}\right) + \sigma_n(\mathbf{x})\phi\left(\frac{m_n(\mathbf{x}) - y_{\max}}{\sigma_n(\mathbf{x})}\right). \quad (12)$$

219 However, by maximizing the  $EI_{\max}$  function (the EI-MAX criterion), only one point for max-  
 220 imization is produced. In order to obtain a batch of  $q$  points, the the first point  $\mathbf{x}_{\max}^{(n+1)}$  can be  
 221 identified by  $\mathbf{x}_{\max}^{(n+1)} = \arg \max_{\mathbf{x} \in \mathbf{x}^I} EI_{\max}(\mathbf{x})$ . The following  $q - 1$  points should be sequentially  
 222 selected by using a modified  $EI_{\max}$  function. In analogy to the  $PEI_{\min}$  function (Eq. (10)), we  
 223 can define the  $PEI_{\max}$  function for the  $q$ -th point such that:

$$PEI_{\max}(\mathbf{x}; \mathbf{x}_{\max}^{(n+1)}, \mathbf{x}_{\max}^{(n+2)}, \dots, \mathbf{x}_{\max}^{(n+q-1)}) = EI_{\max}(\mathbf{x}) \times IF(\mathbf{x}; \mathbf{x}_{\max}^{(n+1)}, \mathbf{x}_{\max}^{(n+2)}, \dots, \mathbf{x}_{\max}^{(n+q-1)}), \quad (13)$$

where the  $IF(\cdot)$  function is defined in Eq. (9). The  $q$ -th point  $\mathbf{x}_{\max}^{(n+q)}$  is obtained by:

$$\mathbf{x}_{\max}^{(n+q)} = \arg \max_{\mathbf{x} \in \mathbf{x}^I} PEI_{\max}(\mathbf{x}; \mathbf{x}_{\max}^{(n+1)}, \mathbf{x}_{\max}^{(n+2)}, \dots, \mathbf{x}_{\max}^{(n+q-1)}).$$

224 *3.2.3. Engine 3: PEI for both minimum and maximum*

225 As we would like to infer both the minimum and maximum simultaneously, rather than in  
 226 a sequential order, promising points for both extrema should be identified within one iteration  
 227 until some predefined criteria are satisfied. Based on the PEI-MIN and PEI-MAX criteria, a  
 228 infill sampling criterion for both minimizing and maximizing the  $g$ -function can be developed.  
 229 This criterion is denoted by PEI-MIN-MAX, and it is served as the third engine.

230 The proposed PEI-MIN-MAX criterion proceeds as follows. The first updating point is  
 231 identified by  $\mathbf{x}_{\min}^{(n+1)} = \arg \max_{\mathbf{x} \in \mathbf{x}^I} EI_{\min}(\mathbf{x})$ , which is used for minimization. Likewise, the sec-  
 232 ond one (the first point for maximization) is computed by maximizing the  $PEI_{\max}(\mathbf{x})$  function,  
 233 i.e.,  $\mathbf{x}_{\max}^{(n+2)} = \arg \max_{\mathbf{x} \in \mathbf{x}^I} PEI_{\max}(\mathbf{x}; \mathbf{x}_{\min}^{(n+1)})$ . The third point (the second for minimization) is  
 234 produced by maximizing the  $PEI_{\min}$  function, i.e.,  $\mathbf{x}_{\min}^{(n+3)} = \arg \max_{\mathbf{x} \in \mathbf{x}^I} PEI_{\min}(\mathbf{x}; \mathbf{x}_{\min}^{(n+1)}, \mathbf{x}_{\max}^{(n+2)})$ ,  
 235 and the fourth one (the second point for maximization) is determined by maximizing the  
 236  $PEI_{\max}$  function, i.e.,  $\mathbf{x}_{\max}^{(n+4)} = PEI_{\max}(\mathbf{x}; \mathbf{x}_{\min}^{(n+1)}, \mathbf{x}_{\max}^{(n+2)}, \mathbf{x}_{\min}^{(n+3)})$ . As the process goes on, a de-  
 237 sired  $q$  ( $\geq 2$ ) updating points can be obtained sequentially ahead of observing their  $g$ -function  
 238 values. Note that one can also start the first point with  $\mathbf{x}_{\max}^{(n+1)}$ , and then generate a set of  $q$   
 239 points  $(\mathbf{x}_{\max}^{(n+1)}, \mathbf{x}_{\min}^{(n+2)}, \mathbf{x}_{\max}^{(n+3)}, \dots)$  following a similar procedure.

240 *3.3. Proposed T-PBGO algorithm*

241 Based on the GP model and T-PEI infill sampling criterion, we propose a T-PBGO algorithm for inter-  
 242 val analysis. The numerical implementation procedure of the proposed T-PBGO algorithm, which is also  
 243 illustrated in Fig. 1, includes the following main steps:

- 244
- 245 **Step 1: Define the problem and initialize the optimization**
- 246 Define the minimization and maximization problem to be solved in terms of its objective  
 247 function  $g(\mathbf{x})$  and feasible region  $\mathbf{x}^I$ , as in Eqs. (2) and (3). Initialize the parameters of the  
 248 proposed T-PBGO method, namely, the initial sample size  $n_0$ , and two thresholds  $\varepsilon_{\min}$  and

249  $\varepsilon_{\max}$ . Details about these parameters and possible numerical values for them are discussed  
250 below.

### 251 **Step 2: Generate an initial training dataset**

252 Generate an initial set of  $n_0$  samples using Latin hypercube sampling (LHS) over  $\mathbf{x}^I$ , denoted by a  $n_0 \times d$   
253 matrix  $\mathbf{X} = \{\mathbf{x}^{(j)}\}_{j=1}^{n_0}$ . Observations of the  $g$ -function at these points can be computed in parallel, which  
254 are denoted by a  $n_0 \times 1$  vector  $\mathbf{y} = \{y^{(j)}\}_{j=1}^{n_0}$  with  $\mathbf{y}^{(j)} = g(\mathbf{x}^{(j)})$ . The initial training dataset is defined as  
255  $\mathcal{D} = \{\mathbf{X}, \mathbf{y}\}$ . Set  $n = n_0$ .

256 As we seek to enlarge the training dataset sequentially, the initial size  $n_0$  should not be chosen too large  
257 and it is usually set as 5-10.

### 258 **Step 3: Construct a GP model for the $g$ -function**

259 Construct a GP model  $\mathcal{GP}(m_n(\mathbf{x}), k_n(\mathbf{x}, \mathbf{x}'))$  for  $y = g(\mathbf{x})$  based on the training dataset  $\mathcal{D}$ . This step  
260 mainly consists of specifying the hyper-parameters by using the maximum likelihood estimation. All the  
261 numerical examples in this study are performed with the *fitrgp* function in Matlab Statistics and Machine  
262 Learning Toolbox.

### 263 **Step 4: Check the predefined criteria and select the engine**

264 In this stage, we first need to check whether the GP has achieved reasonable accuracy at both the  
265 minimum and maximum. If not, the GP should be then improved further, and this improvement means  
266 computing additional points. Thus, it should be clear what kind of additional points is still required, for  
267 minimization, maximization or both. Let  $y_{\min} = \min_{1 \leq j \leq n} y^{(j)}$  and  $y_{\max} = \max_{1 \leq j \leq n} y^{(j)}$  denote the  
268 minimum and maximum values of  $y$  observed so far, respectively. Compute the maxima of  $EI_{\min}(\mathbf{x})$  and  
269  $EI_{\max}(\mathbf{x})$  by:  $\delta y_1 = \max_{\mathbf{x} \in \mathbf{x}^I} EI_{\min}(\mathbf{x})$  and  $\delta y_2 = \max_{\mathbf{x} \in \mathbf{x}^I} EI_{\max}(\mathbf{x})$ . In this study, five criteria consisting  
270 in judging the ratios of the maximum expected improvements (i.e.,  $\delta y_1$  and  $\delta y_2$ ) to the best current minimum  
271 and maximum (i.e.,  $y_{\min}$  and  $y_{\max}$ ) respectively, are given as follows:

272 • **Criterion 1 (Stopping criterion)**. If both  $\frac{\delta y_1}{|y_{\min}|+\delta} < \varepsilon_{\min}$  and  $\frac{\delta y_2}{|y_{\max}|+\delta} < \varepsilon_{\max}$  are satisfied for two  
273 successive iterations, go to **Step 7**; Else, check Criterion 2.

274 • **Criterion 2**. If  $\frac{\delta y_1}{|y_{\min}|+\delta} \geq \varepsilon_{\min}$  and  $\frac{\delta y_2}{|y_{\max}|+\delta} \geq \varepsilon_{\max}$ , this indicates that the GP could be still not

275 accurate enough for estimating both the minimum and maximum and one should go to **Step 5c**; Else, check  
 276 Criterion 3.

277 • **Criterion 3.** If  $\frac{\delta y_1}{|y_{\min}|+\delta} < \varepsilon_{\min}$  and  $\frac{\delta y_2}{|y_{\max}|+\delta} < \varepsilon_{\max}$ , this indicates that the GP could be still not  
 278 accurate enough for both estimating the minimum and maximum (due to potential fake convergence) and  
 279 one should go to **Step 5c**; Else, check Criterion 4.

280 • **Criterion 4.** If  $\frac{\delta y_1}{|y_{\min}|+\delta} \geq \varepsilon_{\min}$  and  $\frac{\delta y_2}{|y_{\max}|+\delta} < \varepsilon_{\max}$ , this indicates that the GP could be still not  
 281 accurate for estimating the minimum one should go to **Step 5a**; Else, check Criterion 5.

282 • **Criterion 5.** If  $\frac{\delta y_1}{|y_{\min}|+\delta} < \varepsilon_{\min}$  and  $\frac{\delta y_2}{|y_{\max}|+\delta} \geq \varepsilon_{\max}$ , this indicates that the GP could be still not  
 283 accurate enough for estimating the maximum one should go to **Step 5b**.

284 In Criteria 1-5,  $\delta$  is a small number to ensure that the denominators are always greater than zero, which  
 285 is specified as  $10^{-6}$  in this study. It should be noted that these two quantities  $\frac{\delta y_1}{|y_{\min}|+\delta}$  and  $\frac{\delta y_2}{|y_{\max}|+\delta}$  play a  
 286 pivotal role for our decision-making. The first one represents the ratio of maximum expected improvement  
 287 for the minimum to the current absolute minimum, while the second one is the ratio of maximum expected  
 288 improvement for the maximum to the current absolute maximum, if  $\delta$  is treated as zero. When the current  
 289 GP model is relatively accurate for both the minimum and maximum, it is expected that these two ratios  
 290 should be very small. Thus, it is appropriate to judge the convergence of the proposed method by monitoring  
 291 these two ratios. According to our experience,  $\varepsilon_{\min}$  and  $\varepsilon_{\max}$  can be set in the order of 0.001.

#### 292 **Step 5a: Identify $q$ updating points for minimization (Engine 1)**

293 Identify  $q$  updating points for minimization by using the PEI-MIN criterion. The first point is selected  
 294 by  $\mathbf{x}_{\min}^{(n+1)} = \arg \max_{\mathbf{x} \in \mathbf{x}^I} EI_{\min}(\mathbf{x})$ , the second one  $\mathbf{x}_{\min}^{(n+2)} = \arg \max_{\mathbf{x} \in \mathbf{x}^I} PEI_{\min}(\mathbf{x}; \mathbf{x}_{\min}^{(n+1)})$ , and the  
 295 third one  $\mathbf{x}_{\min}^{(n+3)} = \arg \max_{\mathbf{x} \in \mathbf{x}^I} PEI_{\min}(\mathbf{x}; \mathbf{x}_{\min}^{(n+1)}, \mathbf{x}_{\min}^{(n+2)})$ , etc. The  $q$  updating points can be denoted by  
 296  $\mathbf{X}_{\text{add}} = \{\mathbf{x}_{\min}^{(n+1)}, \mathbf{x}_{\min}^{(n+2)}, \dots, \mathbf{x}_{\min}^{(n+q)}\}$ . Then, go to **Step 6**.

#### 297 **Step 5b: Identify $q$ updating points for maximization (Engine 2)**

298 Identify  $q$  updating points for maximization by using the PEI-MAX criterion. The first point is selected  
 299 by  $\mathbf{x}_{\max}^{(n+1)} = \arg \max_{\mathbf{x} \in \mathbf{x}^I} EI_{\max}(\mathbf{x})$ , the second one  $\mathbf{x}_{\max}^{(n+2)} = \arg \max_{\mathbf{x} \in \mathbf{x}^I} PEI_{\max}(\mathbf{x}; \mathbf{x}_{\max}^{(n+1)})$ , and the  
 300 third one  $\mathbf{x}_{\max}^{(n+3)} = \arg \max_{\mathbf{x} \in \mathbf{x}^I} PEI_{\max}(\mathbf{x}; \mathbf{x}_{\max}^{(n+1)}, \mathbf{x}_{\max}^{(n+2)})$ , etc. The  $q$  updating points can be denoted by

301  $\mathbf{X}_{\text{add}} = \{\mathbf{x}_{\text{max}}^{(n+1)}, \mathbf{x}_{\text{max}}^{(n+2)}, \dots, \mathbf{x}_{\text{max}}^{(n+q)}\}$ . Then, go to **Step 6**.

302 **Step 5c: Identify  $q$  updating points for both minimization and maximization (Engine 3)**

303 Identify  $q$  updating points for both minimization and maximization by using the PEI-MIN-MAX crite-  
304 rion. The first point is selected by  $\mathbf{x}_{\text{min}}^{(n+1)} = \arg \max_{\mathbf{x} \in \mathbf{x}^I} EI_{\text{min}}(\mathbf{x})$ , the second one  $\mathbf{x}_{\text{max}}^{(n+2)} = \arg \max_{\mathbf{x} \in \mathbf{x}^I} PEI_{\text{max}}(\mathbf{x}; \mathbf{x}_{\text{min}}^{(n+1)})$   
305 and the third one  $\mathbf{x}_{\text{min}}^{(n+3)} = \arg \max_{\mathbf{x} \in \mathbf{x}^I} PEI_{\text{min}}(\mathbf{x}; \mathbf{x}_{\text{min}}^{(n+1)}, \mathbf{x}_{\text{max}}^{(n+2)})$ , etc. The  $q$  updating points can be de-  
306 noted by  $\mathbf{X}_{\text{add}} = \{\mathbf{x}_{\text{min}}^{(n+1)}, \mathbf{x}_{\text{max}}^{(n+2)}, \dots, \mathbf{x}_{\text{max}}^{(n+q)}\}$ . Then, go to **Step 6**.

307 **Step 6: Enrich the training dataset**

308 The  $q$  updating points  $\mathbf{X}_{\text{add}}$  are evaluated on the  $g$ -function in parallel, and the corresponding ob-  
309 servations are denoted by  $\mathbf{y}_{\text{add}} = \{y^{(n+1)}, y^{(n+2)}, \dots, y^{(n+q)}\}$ . The training dataset  $\mathcal{D}$  is enriched by  
310  $\mathcal{D}_{\text{add}} = \{\mathbf{X}_{\text{add}}, \mathbf{y}_{\text{add}}\}$ , i.e.,  $\mathcal{D} = \mathcal{D} \cup \mathcal{D}_{\text{add}}$ . Set  $n = n + q$  and then go to **Step 2**.

311 **Step 7: Record results and end the algorithm**

312 Record  $y_{\text{min}} = \min_{1 \leq j \leq n} y^{(j)}$  and  $y_{\text{max}} = \max_{1 \leq j \leq n} y^{(j)}$  as approximate solutions to the lower and upper  
313 bounds of  $y^I$  respectively, and end the algorithm.

314

315 **In Steps 4 and 5a-5c, the involved optimization problems are solved by a nature-inspired**  
316 **global optimizer, called Teaching-learning-based optimization (TLBO) [42], as they are usually**  
317 **much more cheaper compared to one call of the computational model. As the proposed method**  
318 **is rooted in the classical BGO method, its theoretical analysis may refer to, e.g., [43], which,**  
319 **however, is beyond the scope of the present study.**

320 The proposed method has four major advantages. First, the technique often requires relatively few  $g$ -  
321 function evaluations. This is possible because one can incorporate prior knowledge to explore the design  
322 space. Second, our method allows a high-level parallelization as the proposed T-PEI criterion is compu-  
323 tationally tractable for selecting multiple informative and diverse points. This feature further makes the  
324 method time-saving when parallel computing is available. Third, the proposed method is derivative-free and  
325 directly works with black-boxes, and thus is easy to implement and widely applicable (e.g., no matter the  
326  $g$ -function is linear or non-linear and how large the supports of the input intervals are). Fourth, accurate



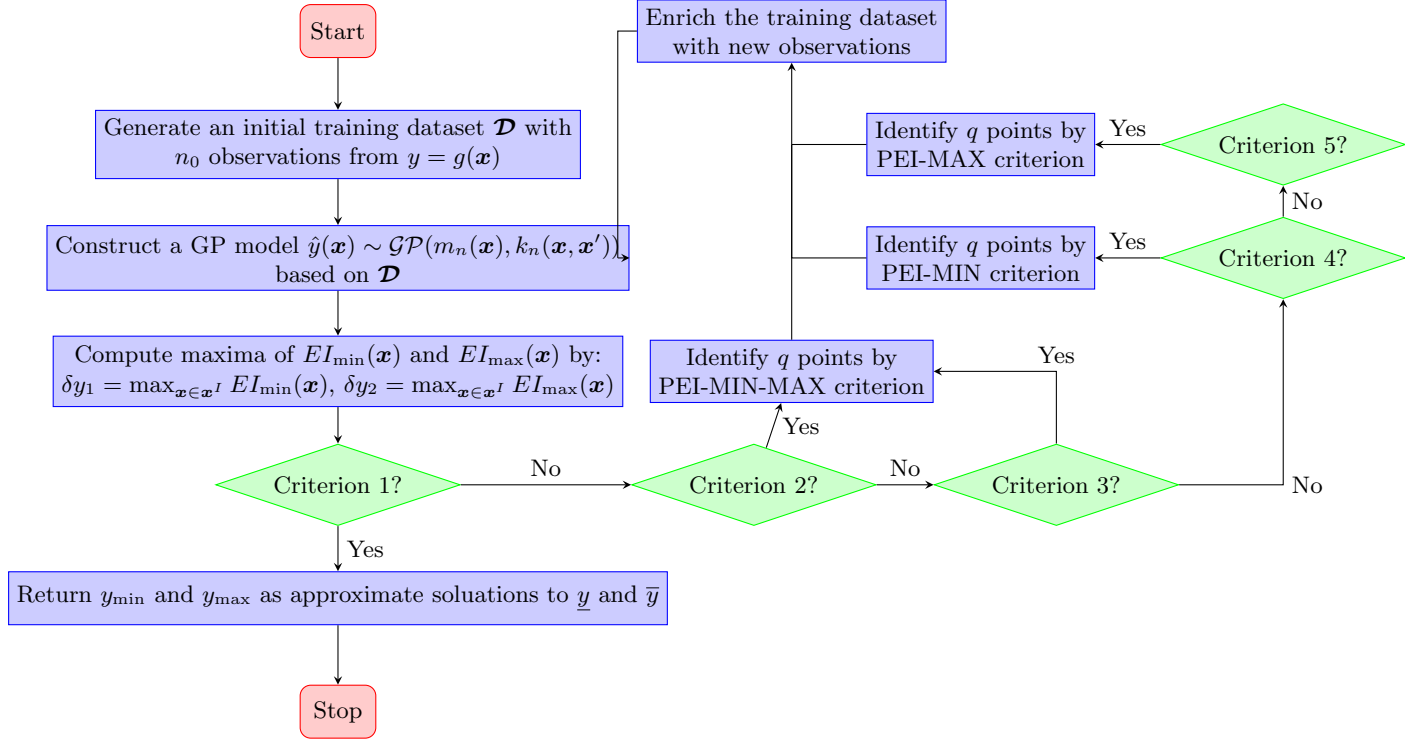


Figure 1: Flowchart of the proposed T-PBGO method.

327 approximate solutions to both lower and upper bounds of model response can be obtained with only one  
 328 single run of the proposed algorithm.

### 329 3.4. Relationship to existing PBGO approaches

330 With the emergence of the classical BGO (originally called efficient global optimization)  
 331 [32], there has been an growing interest to enable its capability of parallel processing. Repre-  
 332 sentative works of PBGO include the  $q$ -EI criterion [44–46], multi-modal EI criterion [47, 48],  
 333 PEI [41], Kriging Believer or Constant Liar strategy [45] and multiple surrogate assisted ap-  
 334 proach [49, 50], etc. The T-PEI criterion in the proposed T-PBGO method can be regarded as  
 335 an improved PEI. The difference between the proposed method and the other PBGO methods  
 336 is significant. The objective of the proposed method is to obtain both the minimum and maxi-  
 337 mum in one single run, while the other methods are only designed for minimum or maximum,  
 338 not both.

## 339 4. Numerical examples

340 In order to illustrate and verify the proposed method, four numerical examples are studied in this section.  
341 These examples cover a wide range of types, from simple test problems to real-world applications. In all  
342 numerical examples, the proposed method is compared with several existing methods in terms of efficiency  
343 and accuracy. Besides, we propose a non-parallel BGO (N-PBGO) (given in [Appendix A](#)) as a potential  
344 competitor for the proposed method, which is also conducted for comparison.

### 345 4.1. Example 1: A one-dimensional test function

The first example consists of a test function with one interval:

$$y = g(x) = (2x - 1)^2 \sin\left(4\pi x - \frac{\pi}{8}\right),$$

346 where  $x \in [0, 1]$ . As can also be seen in [Fig. 2](#), the  $g$ -function is multi-modal and has multiple maxima and  
347 minima.

348 The lower and upper bounds of  $y$  are computed by the analytical method, vertex method, genetic  
349 algorithm, N-PBGO and proposed T-PBGO method ( $n_0 = 5$  and  $\varepsilon_{\min} = \varepsilon_{\max} = 0.002$ ). The results  
350 are summarized in [Table 1](#) together with the total number of function evaluations  $N$ , and the number of  
351 iterations  $N^*$ . Although the vertex method outperforms the other numerical methods in terms of both  $N$   
352 and  $N^*$ , it produces totally wrong estimates for the response bounds. The inaccuracy of the interval method  
353 is caused by its underlying assumption that  $y$  should be monotonic with respect to  $\mathbf{x}$ . As a representative  
354 of nature-inspired optimization algorithms, the genetic algorithm is able to yield accurate results, but at  
355 the expense of large computation cost. The N-PBGO method requires a relatively small number of function  
356 evaluations ( $N = 16$ ), while still providing good results for both the lower and upper bounds. The N-  
357 PBGO method, however, is limited by its non-parallelism. On the contrary, the proposed T-PBGO method  
358 can overcome this limitation by taking advantage of the developed infill sampling criterion (i.e., T-PEI).  
359 Compared to N-PBGO, T-PBGO can significantly reduce the function evaluations in terms of  $N^*$ , while still  
360 maintaining high accuracy. In addition, it also can be found that  $N^*$  gradually decreases with the increase  
361 of  $q$ , and remains the same when  $q = 8, 10$ , though  $N$  also increases non-monotonously.

Table 1: Interval analysis for Example 1 by different methods.

Method		Lower bound	Upper bound	$N$	$N^*$	Reference
Exact solution		-0.7081	0.5197	-	-	-
Vertex method ( $q = 2$ )		-0.3827	-0.3827	2	1	[26]
Genetic algorithm ( $q = 10$ )		-0.7081	0.5197	$520 + 520 = 1040$	104	[51]
N-PBGO ( $q = 1$ )		-0.7081	0.5197	$5 + 6 + 5 = 16$	16	Appendix A
	$q = 2$	-0.7081	0.5197	$5 + 8 = 13$	7	-
	$q = 4$	-0.7081	0.5197	$5 + 16 = 21$	6	-
Proposed method (T-PBGO)	$q = 6$	-0.7081	0.5197	$5 + 24 = 29$	5	-
	$q = 8$	-0.7081	0.5197	$5 + 24 = 29$	4	-
	$q = 10$	-0.7081	0.5197	$5 + 30 = 35$	4	-

Note:  $N$  = the total number of  $g$ -function evaluations, and  $N^*$  = the number of iterations

362 To visually illustrate the proposed method, one special case is considered here (i.e.,  $q = 4$ ). It can be  
 363 observed from Fig. 2 that the proposed method gradually approaches to the exact bounds as the iterative  
 364 process goes on. Besides, these added points are more densely distributed around the global minimum and  
 365 maximum, and thereby informative for our purposes.

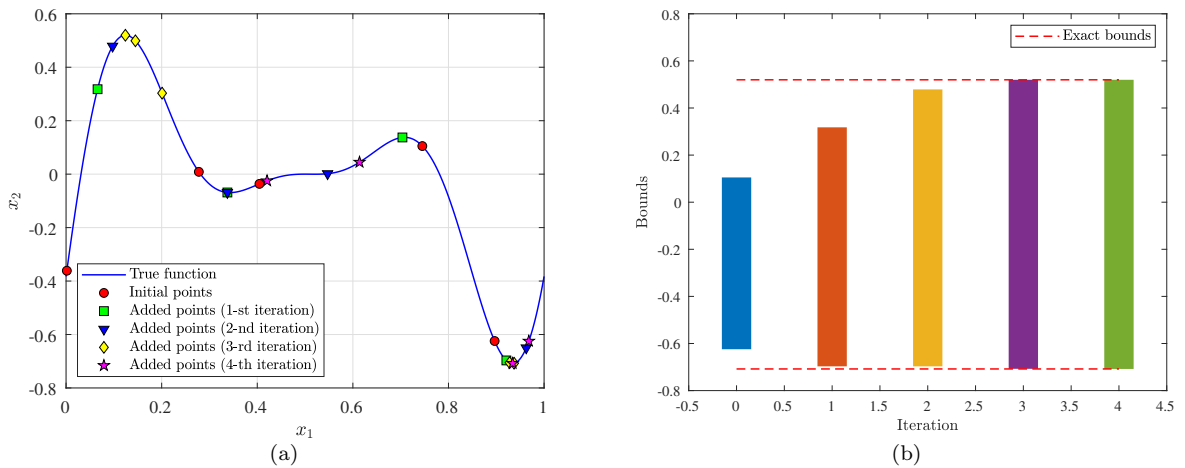


Figure 2: Illustration of the proposed method ( $q = 4$ ) in Example 1: (a) True function, initial points and added points identified by T-PEI criterion; (b) Exact bounds and approximate bounds after each iteration.

The second example takes a test function with two intervals [21]:

$$y = g(\mathbf{x}) = (1.5x_1 - 2)^2 - (x_2 - 3)^2 + x_1x_2 + 10 \sin(2\pi x_1) + 10 \sin(2\pi x_2),$$

367 where  $x_1, x_2 \in [2, 5]$ . As shown in Fig. 3, the test function is highly nonlinear and has several  
 368 local optima over the prescribed region.

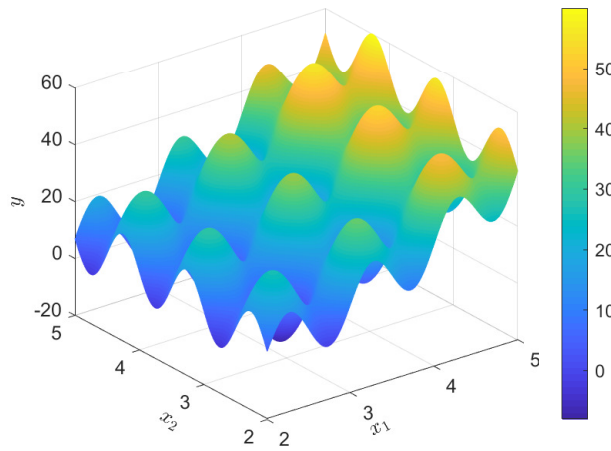


Figure 3: Plot of the two-dimensional test function in Example 2.

369 The lower and upper bounds of  $y$  are computed by several methods, as listed in Table  
 370 2. The exact response bounds of  $y$  are obtained as  $-8.10$  and  $59.95$ . The genetic algorithm  
 371 can yield accurate results, but at the expense of 4000  $g$ -function evaluations. Although the  
 372 classical vertex method requires the minimum number of  $g$ -function evaluations among all the  
 373 numerical methods, it gives completely wrong estimates for the lower and upper bounds. At  
 374 the cost of 6912  $g$ -function calls (the largest among all the numerical methods), the subinterval  
 375 method is able to produce acceptable results. The subinterval decomposition analysis method  
 376 yields close results to these of the subinterval method, while requires significantly less  $g$ -  
 377 function evaluations. For the N-PGBO method, fairly good results can be produced using a  
 378 total number of 74  $g$ -function evaluations, and 65 iterations. The proposed T-PBGO method

379 ( $n_0 = 10$ ,  $\varepsilon_{\min} = 0.002$  and  $\varepsilon_{\max} = 0.001$ ) is capable of generating quite accurate lower and upper  
 380 bounds, while reducing the number of iterations down to 9 when  $q = 8$ .

Table 2: Interval analysis results for Example 2 by different methods.

Method	Lower bound	Upper bound	$N$	$N^*$	Reference
Exact solution	-8.10	59.95	-	-	-
Genetic algorithm	-8.10	59.95	4000	-	Tab. 7 in [21]
Vertex method ( $q = 4$ )	4.00	51.25	4	1	[26]
Subinterval method	-8.70	60.39	6912	-	Tab. 7 in [21]
Subinterval decomposition analysis	-8.55	58.81	97	-	Tab. 7 in [21]
N-PBGO ( $q = 1$ )	-8.01	59.92	$10 + 42 + 22 = 74$	65	<a href="#">Appendix A</a>
	$q = 2$ -8.08	59.94	$10 + 58 = 68$	30	-
	$q = 4$ -8.08	59.94	$10 + 72 = 82$	19	-
Proposed method (T-PBGO)	$q = 6$ -8.09	59.93	$10 + 72 = 82$	13	-
	$q = 8$ -8.10	59.94	$10 + 80 = 90$	9	-
	$q = 10$ -8.10	59.93	$10 + 90 = 100$	10	-

### 381 4.3. Example 3: A transmission tower subjected to wind loads

This example consists of a transmission tower subjected to wind loads (shown in Fig. 4), which is modified from Ref. [52]. The tower is modelled as a three-dimensional (3D) truss structure with 24 joints and 80 elements in OpenSees. Three kinds of members, i.e., columns, diagonal members and horizontal members, are included in the model, the cross-sectional area of which are denoted as  $A_1$ ,  $A_2$  and  $A_3$ , respectively. The geometry of the model is shown in Fig. 4(a). The wind effect acting on the tower is simplified to four equivalent static loads at the top four nodes, and inclined by  $\theta^\circ$  relative to the  $x$ -axis (Fig. 4(b)). The constitutive law of the steel material adopts the bi-linear model, as depicted in Fig. 4(c). Eight interval variables are included in the 3D truss model, which are described in Table 3. The response of interest is

defined as the horizontal displacement of node A, i.e.,

$$y = g(P, \theta, F_y, E, b, A_1, A_2, A_3) = \sqrt{u_{A,x}^2 + u_{A,y}^2},$$

382 where  $u_{A,x}$  and  $u_{A,y}$  denote the displacements of node A in  $x$  and  $y$  directions, respectively.

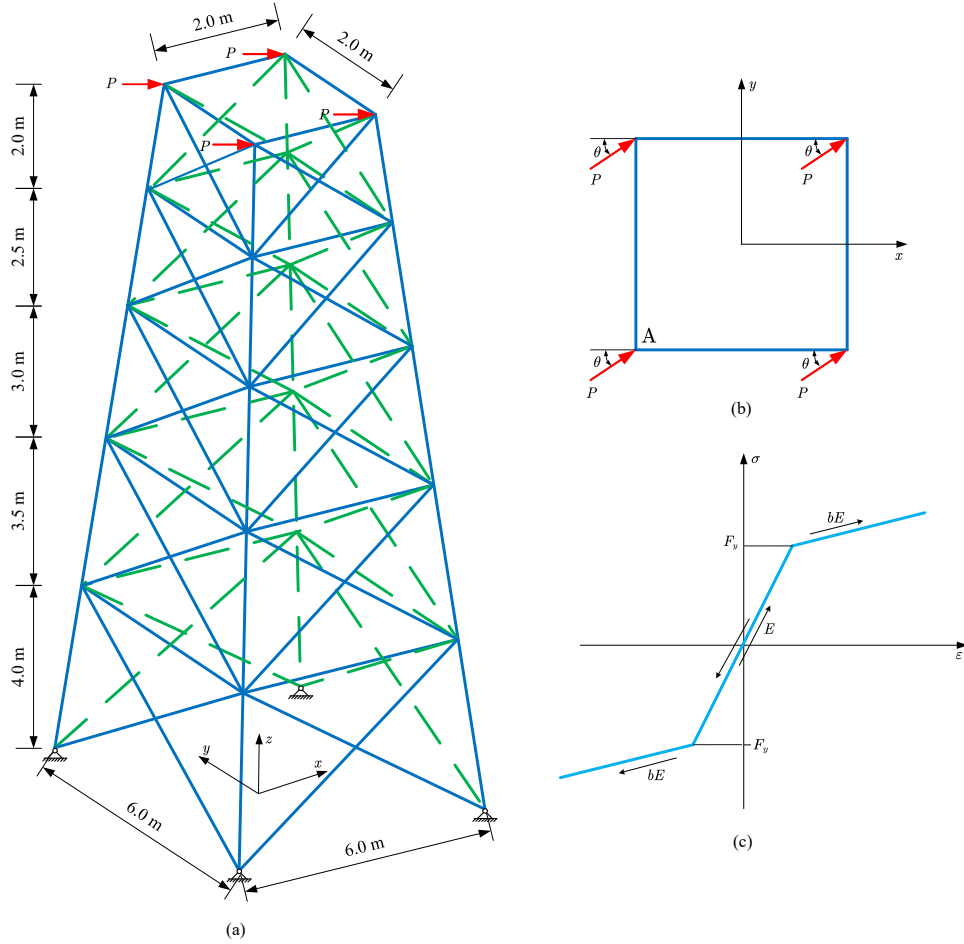


Figure 4: A transmission tower subject to wind loads: (a) 3D truss model; (b) loading at the top of tower; (c) bi-linear constitutive model.

383 The bounds of  $y$  are solved by several methods, and the results are summarized in Table 4. The particle  
 384 swarm optimization ( $q = 10$ ) is used to provide reference results for the bounds. For the proposed T-PBGO  
 385 method, we set the user-specified parameters as:  $n_0 = 10$ ,  $\epsilon_{\min} = 0.002$  and  $\epsilon_{\max} = 0.001$ . The vertex  
 386 method requires 256  $g$ -function calls, which, however, greatly underestimates the upper bound. Both N-  
 387 PBGO and T-PBGO can give close results to these of particle swarm optimization. The N-PBGO method is

Table 3: Interval variables for Example 3.

Variable	Description	Interval	Unit
$P$	Wind load	[100, 200]	kN
$\theta$	Angle between the load direction and the $x$ -axis	$[-45, 45]$	$^\circ$
$F_y$	Yield strength of steel	[300, 400]	MPa
$E$	Young's modulus of steel	$[1.8, 2.4] \times 10^5$	MPa
$b$	Strain hardening ratio	[0.015, 0.025]	-
$A_1$	Cross-sectional area of the column members	[4000, 5000]	mm <sup>2</sup>
$A_2$	Cross-sectional area of the diagonal members	[3000, 4000]	mm <sup>2</sup>
$A_3$	Cross-sectional area of the horizontal members	[2000, 3000]	mm <sup>2</sup>

388 computationally advantageous in terms of  $N$  among all methods, while the proposed T-PBGO can further  
389 reduce  $N^*$  by taking advantage of its parallelism.

Table 4: Interval analysis results for Example 3 by different methods.

Method		Lower bound/mm	Upper bound/mm	$N$	$N^*$	Reference
Particle swarm optimization ( $q = 10$ )		11.9592	57.2421	$1920 + 3840 = 5760$	576	[51]
Vertex method ( $q = 10$ )		11.9592	44.3887	256	25.60	[26]
N-PBGO ( $q = 1$ )		11.9592	57.2421	$10 + 9 + 5 = 24$	24	Appendix A
	$q = 2$	11.9592	57.2403	$10 + 22 = 32$	16	-
	$q = 4$	11.9592	57.2421	$10 + 28 = 38$	10	-
Proposed method (T-PBGO)	$q = 6$	11.9592	57.2372	$10 + 36 = 46$	8	-
	$q = 8$	11.9592	57.2421	$10 + 40 = 50$	7	-
	$q = 10$	11.9760	57.2388	$10 + 60 = 70$	7	-

#### 390 4.4. Example 4: A spatial frame with viscous dampers subjected to earthquake

The last example considers a spatial frame with viscous dampers subjected to earthquake, as shown in Fig. 5. The 3-D finite element model is developed in OpenSees, the geometry of which can be found in

Fig. 5(a). Each beam/column member is modelled with an elastic beam-column element with cross section IPE270/IPB300 (Fig. 5(b)/(c)). For each viscous damper (see Fig. 5(d)), a two-node link element is used with the viscous damper material. We only consider the self weight as the mass source for the columns, while for beams the mass source is determined based on “self weight + dead load + 0.2 live load”. The structure is subjected to a base acceleration corresponding to the N-S component of the El-Centro 1940 earthquake, as shown in 5(e). The ground motion is applied along the direction with a rotation angle  $\theta^\circ$  with respect to the  $y$ -axis (Fig. 5(a)). As summarized in Table 5, eleven interval variables are involved in this example. Of interest is the maximum horizontal displacement of node A, i.e.,

$$y = g(\theta, AF, DL, LL, K_D, C_D, \alpha, \rho, E, v, \zeta) = \max_t \sqrt{u_{A,x}^2(t) + u_{A,y}^2(t)},$$

391 where  $u_{A,x}(t)$  and  $u_{A,y}(t)$  denote the displacements of node A in  $x$  and  $y$  directions, respectively.

Table 5: Interval variables for Example 4.

Variable	Description	Interval	Unit
$\theta$	Angle between the earthquake direction and the $y$ -axis	$[-45, 45]$	$^\circ$
$AF$	Amplification factor of the earthquake ground motion	$[0.5, 1.5]$	-
$DL$	Floor dead load	$[4, 5]$	$\text{kN/m}^2$
$LL$	Floor live load	$[2, 3]$	$\text{kN/m}^2$
$K_D$	Axial Stiffness of the viscous damper	$[3, 4] \times 10^4$	$\text{kN/m}$
$C_D$	Damping coefficient of the viscous damper	$[20, 30]$	$\text{kN(s/m)}^\alpha$
$\alpha$	Velocity exponent	$[0.2, 0.4]$	-
$\rho$	Density of steel	$[7.8, 7.9] \times 10^3$	$\text{kg/m}^3$
$E$	Young’s modulus of steel	$[1.8, 2.2] \times 10^5$	$\text{MPa}$
$v$	Poisson’s ratio	$[0.25, 0.30]$	-
$\zeta$	Damping ratio	$[0.02, 0.04]$	-

392 The bounds of the model response  $y$  are computed by the particle swarm optimization, vertex method,  
393 N-PBGO and T-PBGO ( $n_0 = 10$ ,  $\varepsilon_{\min} = 0.002$  and  $\varepsilon_{\max} = 0.001$ ), and the results are summarized in Table  
394 6. The reference solution is taken from the particle swarm optimization method. The vertex method is able



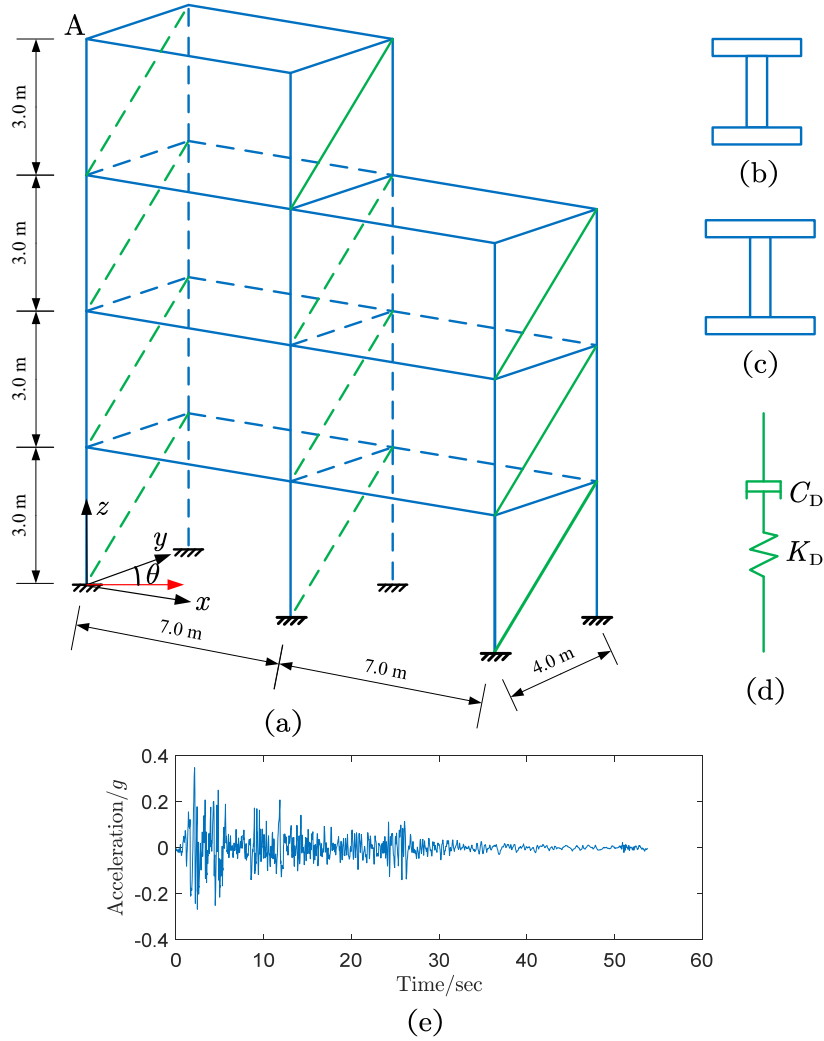


Figure 5: A spatial frame with viscous dampers subject to earthquake: (a) 3D frame model; (b) IPE270 for beams; (c) IPB300 for columns; (4) Viscous Damper; (e) N-S component of El Centro earthquake (1940)

395 to produce good estimates, but requires a large number of  $g$ -function evaluations ( $N = 2048$  and  $N^* = 204.8$ )  
 396 in this example. Compared to the N-PBGO method and vertex method, the proposed T-PBGO method can  
 397 significantly reduce the number of  $g$ -function calls per core, though the total number of  $g$ -function calls may  
 398 increase (e.g.,  $q = 4, 8$ ) relative to the N-PBGO method. Besides, the proposed method still gives desirable  
 399 results for the response bounds. It should be emphasized that  $N^*$  does not decrease monotonically as  $q$   
 400 increases. This means that there may be an optimal parallelization level  $q$  that minimizes  $N^*$ , e.g.,  $q = 6$  in  
 401 the example.

Table 6: Interval analysis results for Example 4 by different methods.

Method	Lower bound/mm	Upper bound/mm	$N$	$N^*$	Reference
Particle swarm optimization ( $q = 10$ )	11.9762	137.4651	$3000 + 2400 = 5400$	540	[51]
Vertex method ( $q = 10$ )	12.0084	137.4651	2048	204.8	[26]
N-PBGO ( $q = 1$ )	12.0929	137.3746	$10 + 14 + 4 = 28$	28	Appendix A
	$q = 2$ 12.0483	137.4651	$10 + 14 = 24$	12	-
	$q = 4$ 12.0084	137.2062	$10 + 24 = 34$	9	-
Proposed method (T-PBGO)	$q = 6$ 12.0489	137.4651	$10 + 18 = 28$	5	-
	$q = 8$ 12.0063	137.4651	$10 + 32 = 42$	6	-

#### 4.5. Final remarks

In practical applications, the  $g$ -function can be rather expensive-to-evaluate and the computational budget is limited. In such cases, one may need to prespecify optimal values for the parameters  $n_0$ ,  $q$ ,  $\varepsilon_{\min}$  and  $\varepsilon_{\max}$  before running the proposed method in order to save the computational time, while remaining a desired level of accuracy. As a rule of thumb, the initial sample size  $n_0$  can be set as 10. As observed in the four numerical examples, the number of iterations  $N^*$  does not decrease monotonically with  $q$  and takes its minimum value when  $q = 8$  in most cases. Therefore,  $q = 8$  is recommended in case that at least 8 cores are available. The two thresholds  $\varepsilon_{\min}$  and  $\varepsilon_{\max}$  not only influence the the efficiency of the proposed method, but also the accuracy, The smaller  $\varepsilon_{\min}$  and  $\varepsilon_{\max}$  are, the proposed method usually requires more iterations and more accurate results can be obtained. According to our experience,  $\varepsilon_{\min} = 0.002$  and  $\varepsilon_{\max} = 0.002$  can be adopted.

## 5. Conclusions

In this study, a triple-engine parallel Bayesian global optimization (T-PBGO) method is proposed for efficient interval numerical analysis, especially when the computational model is a expensive-to-evaluate black box. The advancement of the proposed method lies in utilizing the Gaussian process (GP,

418 also known as Kriging) prior for the expensive black-box  $g$ -function and an acquisition function (or infill  
419 sampling criterion) that can suggest promising points to be evaluated next. To order to make full use of prior  
420 knowledge and parallel computing, the main contribution of this paper is the development of a multi-points  
421 selection strategy, called ‘triple-engine pseudo expected improvement’ (T-PEI), which can select a batch of  
422 informative and diversity points for minimization and/or maximization at each iteration. Four numerical  
423 examples are investigated to demonstrate the proposed method. The main advantages of T-PBGO can be  
424 summarized as follows:

- 425 (i) The proposed method usually requires less  $g$ -function evaluations to achieve the same accuracy com-  
426 pared to non-Bayesian methods, due to its ability to exploit prior knowledge;
- 427 (ii) Compared to N-PBGO, T-PBGO allows for identifying multiple points at each iteration, and hence  
428 could be more efficient when parallel computing is available;
- 429 (iii) The developed method is non-intrusive in nature (directly works with black-box problems), and there-  
430 fore easy-to-implement and broadly applicable;
- 431 (iv) Both lower and upper bounds can be obtained with one single run of the proposed method.

432 However, the proposed method still has several major limitations. First, T-PBGO typically works only  
433 well in low dimensions (typically,  $d < 20$ ), and for high-dimensional problems new developments are needed.  
434 Second, as the parallelization level  $q$  and the size of training dataset increase, optimizing the T-PEI criterion  
435 can be time-consuming. Third, only the bounds of a single model response can be captured by the proposed  
436 method in its current form. Future works can be done along these directions.

#### 437 **Declaration of competing interest**

438 The authors declare that they have no known competing financial interests or personal relationships that  
439 could have appeared to influence the work reported in this paper.

440 **Acknowledgments**

441 Chao Dang is mainly supported by China Scholarship Council (CSC). Pengfei Wei is grateful to the  
442 support from the National Natural Science Foundation of China (grant no. 51905430 and 72171194). Marcos  
443 Valdebenito acknowledges the support by ANID (National Agency for Research and Development, Chile)  
444 under its program FONDECYT, grant number 1180271. Chao Dang, Pengfei Wei and Michael Beer also  
445 would like to appreciate the support of Sino-German Mobility Program under grant number M-0175.

446 **Appendix A. Non-parallel Bayesian global optimization**

447 The traditional Bayesian global optimization is sequential in nature, which means that only one update  
448 point is identified at each iteration. Therefore, it cannot take advantage of parallelism. Besides, finding the  
449 minimum and maximum of a function is typically treated as two separate optimization problems. However,  
450 this is not advisable when computational efficiency is of great concern. That is because that the observations  
451 obtained when searching the minimum can be reused to speed up searching the maximum, and vice versa.  
452 This strategy is adopted in this study as a potential competitor to the proposed method, and we simply call  
453 it non-parallel Bayesian global optimization (N-PBGO). The main procedure of N-PBGO is summarized as  
454 follows:

455

456 **Step A.1: Generate an initial training dataset**

457 Generate an initial set of  $n_0$  samples using LHS over  $\mathbf{x}^I$ , denoted by a  $n_0 \times d$  matrix  $\mathbf{X} = \{\mathbf{x}^{(j)}\}_{j=1}^{n_0}$ .  
458 Observations of the  $g$ -function at these points can be computed in parallel, which are denoted by a  $n_0 \times 1$   
459 vector  $\mathbf{y} = \{y^{(j)}\}_{j=1}^{n_0}$  with  $y^{(j)} = g(\mathbf{x}^{(j)})$ . The initial training dataset can be written as  $\mathcal{D} = \{\mathbf{X}, \mathbf{y}\}$ . Set  
460  $n = n_0$ .

461 **Step A.2: Construct a GP model**

462 Construct a GP model  $\mathcal{GP}(m_n(\mathbf{x}), k_n(\mathbf{x}, \mathbf{x}'))$  based on the initial training dataset  $\mathcal{D}$ . This step mainly  
463 consists of choosing the hyper-parameters by using the maximum likelihood estimation. All the numerical

464 examples in this study are performed with the *fitrgp* function in Matlab Statistics and Machine Learning  
465 Toolbox.

466 **Step A.3: Compute maximum of  $EI_{\min}(\mathbf{x})$**

467 Let  $y_{\min} = \min_{1 \leq j \leq n} y^{(j)}$  denote the minimum value of  $y$  observed so far, respectively. Compute the  
468 maximum of  $EI_{\min}(\mathbf{x})$  by  $\delta y_1 = \max_{\mathbf{x} \in \mathbf{x}'} EI_{\min}(\mathbf{x})$ .

469 **Step A.4: Check stopping criterion for minimization**

470 if  $\frac{\delta y_1}{|y_{\min}| + \delta} < \varepsilon_{\min}$  is satisfied for two successive times, go to **Step A.7**; Otherwise, go to **Step A.5**.

471 **Step A.5: Identify one point by EI-MIN criterion**

472 Identify the next point to evaluate by  $\mathbf{x}_{\min}^{(n+1)} = \arg \max_{\mathbf{x} \in \mathbf{x}'} EI_{\min}(\mathbf{x})$ .

473 **Step A.6: Enrich the training dataset**

474 Compute the corresponding  $g$ -function value at the identified point at  $\mathbf{x}_{\min}^{(n+1)}$ , i.e.,  $y^{(n+1)} = g(\mathbf{x}_{\min}^{(n+1)})$ .  
475 Enrich the training dataset  $\mathcal{D}$  with  $(\mathbf{x}_{\min}^{(n+1)}, y^{(n+1)})$ . Set  $n = n + 1$ , and go to **Step A.2**.

476 **Step A.7: Compute maximum of  $EI_{\max}(\mathbf{x})$**

477 Let  $y_{\max} = \max_{1 \leq j \leq n} y^{(j)}$  denote the maximum value of  $y$  observed so far, respectively. Compute the  
478 maxima of  $EI_{\max}(\mathbf{x})$  by  $\delta y_2 = \max_{\mathbf{x} \in \mathbf{x}'} EI_{\max}(\mathbf{x})$ .

479 **Step A.8: Check stopping criterion for maximization**

480 if  $\frac{\mu_{\max}}{|y_{\max}| + \delta} < \varepsilon_{\max}$  is satisfied for two successive times, go to **Step A.12**; Otherwise, go to **Step A.9**.

481 **Step A.9: Identify one point by EI-MAX criterion**

482 Identify the next point to evaluate by  $\mathbf{x}_{\max}^{(n+1)} = \arg \max_{\mathbf{x} \in \mathbf{x}'} EI_{\max}(\mathbf{x})$ .

483 **Step A.10: Enrich the training dataset**

484 Compute the corresponding  $g$ -function value at the identified point at  $\mathbf{x}_{\max}^{(n+1)}$ , i.e.,  $y^{(n+1)} = g(\mathbf{x}_{\max}^{(n+1)})$ .  
485 Enrich the training dataset  $\mathcal{D}$  with  $(\mathbf{x}_{\max}^{(n+1)}, y^{(n+1)})$ . Set  $n = n + 1$ .

486 **Step A.11: Construct a GP model**

487 Construct a GP model  $\mathcal{GP}(m_n(\mathbf{x}), k_n(\mathbf{x}, \mathbf{x}'))$  based on the initial training dataset  $\mathcal{D}$ , and go to **Step**  
488 **A.7**.

489 **Step A.12: End the algorithm**

490 Take  $y_{\min} = \min_{1 \leq j \leq n} y^{(j)}$  and  $y_{\max} = \max_{1 \leq j \leq n} y^{(j)}$  as approximate solutions to the lower and upper  
491 bounds of  $y$  respectively, and end the algorithm.

492

493 In the above steps, TLBO is used for all optimization problems. Besides, for fair comparison the user-  
494 specified parameters ( $n_0$ ,  $\delta$ ,  $\varepsilon_{\min}$  and  $\varepsilon_{\max}$ ) are set according to the proposed method in all numerical  
495 examples.

## 496 References

- 497 [1] J. Stoer, R. Bulirsch, Introduction to numerical analysis, Vol. 12, Springer Science & Business Media, 2013.
- 498 [2] J. C. Helton, J. D. Johnson, W. L. Oberkampf, An exploration of alternative approaches to the representation of uncertainty  
499 in model predictions, Reliability Engineering & System Safety 85 (1-3) (2004) 39–71. doi:<https://doi.org/10.1016/j.ress.2004.03.025>.
- 500
- 501 [3] M. Beer, S. Ferson, V. Kreinovich, Imprecise probabilities in engineering analyses, Mechanical Systems and Signal Pro-  
502 cessing 37 (1-2) (2013) 4–29. doi:<https://doi.org/10.1016/j.ymsp.2013.01.024>.
- 503 [4] T. Augustin, F. P. Coolen, G. De Cooman, M. C. Troffaes, Introduction to imprecise probabilities, John Wiley & Sons,  
504 2014.
- 505 [5] M. Faes, D. Moens, Recent trends in the modeling and quantification of non-probabilistic uncertainty, Archives of Com-  
506 putational Methods in Engineering 27 (3) (2020) 633–671. doi:<https://doi.org/10.1007/s11831-019-09327-x>.
- 507 [6] C. Jiang, X. Han, G. Lu, J. Liu, Z. Zhang, Y. Bai, Correlation analysis of non-probabilistic convex model and corresponding  
508 structural reliability technique, Computer Methods in Applied Mechanics and Engineering 200 (33-36) (2011) 2528–2546.  
509 doi:<https://doi.org/10.1016/j.cma.2011.04.007>.
- 510 [7] R. E. Moore, Methods and applications of interval analysis, SIAM, 1979.
- 511 [8] C. Jiang, Q. Zhang, X. Han, J. Liu, D. Hu, Multidimensional parallelepiped model—a new type of non-probabilistic  
512 convex model for structural uncertainty analysis, International Journal for Numerical Methods in Engineering 103 (1)  
513 (2015) 31–59. doi:<https://doi.org/10.1002/nme.4877>.
- 514 [9] B. Ni, C. Jiang, X. Han, An improved multidimensional parallelepiped non-probabilistic model for structural uncertainty  
515 analysis, Applied Mathematical Modelling 40 (7-8) (2016) 4727–4745.
- 516 [10] C. Jiang, C.-M. Fu, B.-Y. Ni, X. Han, Interval arithmetic operations for uncertainty analysis with correlated interval  
517 variables, Acta Mechanica Sinica 32 (4) (2016) 743–752. doi:<https://doi.org/10.1007/s10409-015-0525-3>.
- 518 [11] M. Faes, D. Moens, Multivariate dependent interval finite element analysis via convex hull pair constructions and the

- 519 extended transformation method, *Computer Methods in Applied Mechanics and Engineering* 347 (2019) 85–102. doi:  
520 <https://doi.org/10.1016/j.cma.2018.12.021>.
- 521 [12] M. Faes, D. Moens, On auto-and cross-interdependence in interval field finite element analysis, *International Journal for*  
522 *Numerical Methods in Engineering* 121 (9) (2020) 2033–2050. doi:<https://doi.org/10.1002/nme.6297>.
- 523 [13] D. Wu, W. Gao, Hybrid uncertain static analysis with random and interval fields, *Computer Methods in Applied Mechanics*  
524 *and Engineering* 315 (2017) 222–246. doi:<https://doi.org/10.1016/j.cma.2016.10.047>.
- 525 [14] A. Sofi, E. Romeo, O. Barrera, A. Cocks, An interval finite element method for the analysis of structures with spatially  
526 varying uncertainties, *Advances in Engineering Software* 128 (2019) 1–19. doi:[https://doi.org/10.1016/j.advengsoft.](https://doi.org/10.1016/j.advengsoft.2018.11.001)  
527 [2018.11.001](https://doi.org/10.1016/j.advengsoft.2018.11.001).
- 528 [15] I. Elishakoff, Y. Miglis, Novel parameterized intervals may lead to sharp bounds, *Mechanics Research Communications* 44  
529 (2012) 1–8. doi:<https://doi.org/10.1016/j.mechrescom.2012.04.004>.
- 530 [16] I. Elishakoff, K. Thakkar, Overcoming overestimation characteristic to classical interval analysis, *AIAA Journal* 52 (9)  
531 (2014) 2093–2097. doi:<https://doi.org/10.2514/1.J053152>.
- 532 [17] G. Manson, Calculating frequency response functions for uncertain systems using complex affine analysis, *Journal of Sound*  
533 *and Vibration* 288 (3) (2005) 487–521. doi:<https://doi.org/10.1016/j.jsv.2005.07.004>.
- 534 [18] G. Muscolino, A. Sofi, Stochastic analysis of structures with uncertain-but-bounded parameters via improved interval  
535 analysis, *Probabilistic Engineering Mechanics* 28 (2012) 152–163. doi:[https://doi.org/10.1016/j.probengmech.2011.](https://doi.org/10.1016/j.probengmech.2011.08.011)  
536 [08.011](https://doi.org/10.1016/j.probengmech.2011.08.011).
- 537 [19] Z. Qiu, L. Ma, X. Wang, Non-probabilistic interval analysis method for dynamic response analysis of nonlinear systems  
538 with uncertainty, *Journal of Sound and Vibration* 319 (1-2) (2009) 531–540. doi:[https://doi.org/10.1016/j.jsv.2008.](https://doi.org/10.1016/j.jsv.2008.06.006)  
539 [06.006](https://doi.org/10.1016/j.jsv.2008.06.006).
- 540 [20] Z. Deng, Z. Guo, X. Zhang, Non-probabilistic set-theoretic models for transient heat conduction of thermal protection  
541 systems with uncertain parameters, *Applied Thermal Engineering* 95 (2016) 10–17. doi:[https://doi.org/10.1016/j.](https://doi.org/10.1016/j.applthermaleng.2015.10.152)  
542 [applthermaleng.2015.10.152](https://doi.org/10.1016/j.applthermaleng.2015.10.152).
- 543 [21] C. Fu, L. Cao, J. Tang, X. Long, A subinterval decomposition analysis method for uncertain structures with large  
544 uncertainty parameters, *Computers & Structures* 197 (2018) 58–69. doi:[https://doi.org/10.1016/j.compstruc.2017.](https://doi.org/10.1016/j.compstruc.2017.12.001)  
545 [12.001](https://doi.org/10.1016/j.compstruc.2017.12.001).
- 546 [22] M. Valdebenito, C. Pérez, H. Jensen, M. Beer, Approximate fuzzy analysis of linear structural systems applying intervening  
547 variables, *Computers & Structures* 162 (2016) 116–129. doi:<https://doi.org/10.1016/j.compstruc.2015.08.020>.
- 548 [23] M. A. Valdebenito, H. A. Jensen, P. Wei, M. Beer, A. T. Beck, Application of a reduced order model for fuzzy analysis  
549 of linear static systems, *ASCE-ASME Journal of Risk and Uncertainty in Engineering Systems, Part B: Mechanical*  
550 *Engineering* 7 (2) (2021) 020904.
- 551 [24] J. Wu, Z. Luo, Y. Zhang, N. Zhang, L. Chen, Interval uncertain method for multibody mechanical systems using Chebyshev

- 552 inclusion functions, *International Journal for Numerical Methods in Engineering* 95 (7) (2013) 608–630. doi:<https://doi.org/10.1002/nme.4525>.
- 553
- 554 [25] J. Wu, Y. Zhang, L. Chen, Z. Luo, A Chebyshev interval method for nonlinear dynamic systems under uncertainty, *Applied*  
555 *Mathematical Modelling* 37 (6) (2013) 4578–4591. doi:<https://doi.org/10.1016/j.apm.2012.09.073>.
- 556 [26] W. Dong, H. C. Shah, Vertex method for computing functions of fuzzy variables, *Fuzzy sets and Systems* 24 (1) (1987)  
557 65–78. doi:[https://doi.org/10.1016/0165-0114\(87\)90114-X](https://doi.org/10.1016/0165-0114(87)90114-X).
- 558 [27] Z. Qiu, Y. Xia, J. Yang, The static displacement and the stress analysis of structures with bounded uncertainties using  
559 the vertex solution theorem, *Computer Methods in Applied Mechanics and Engineering* 196 (49-52) (2007) 4965–4984.  
560 doi:<https://doi.org/10.1016/j.cma.2007.06.022>.
- 561 [28] R. R. Callens, M. G. Faes, D. Moens, Interval analysis using multilevel quasi-monte carlo, in: *International Workshop on*  
562 *Reliable Engineering Computing (REC2021)*, Vol. 9, International Workshop on Reliable Engineering Computing, 2021,  
563 pp. 53–67.
- 564 [29] R. R. Callens, M. G. Faes, D. Moens, Multilevel quasi-monte carlo for interval analysis, *International Journal for Uncer-*  
565 *tainty Quantification (Accepted for Publication)*.
- 566 [30] F. Biondini, F. Bontempi, P. G. Malerba, Fuzzy reliability analysis of concrete structures, *Computers & structures* 82 (13-  
567 14) (2004) 1033–1052. doi:<https://doi.org/10.1016/j.compstruc.2004.03.011>.
- 568 [31] L. Catalo, Genetic anti-optimization for reliability structural assessment of precast concrete structures, *Computers &*  
569 *Structures* 82 (13-14) (2004) 1053–1065. doi:<https://doi.org/10.1016/j.compstruc.2004.03.018>.
- 570 [32] D. R. Jones, M. Schonlau, W. J. Welch, Efficient global optimization of expensive black-box functions, *Journal of Global*  
571 *Optimization* 13 (4) (1998) 455–492. doi:<https://doi.org/10.1023/A:1008306431147>.
- 572 [33] M. De Munck, D. Moens, W. Desmet, D. Vandepitte, An efficient response surface based optimisation method for non-  
573 deterministic harmonic and transient dynamic analysis, *Computer Modeling in Engineering & Sciences* 47 (2) (2009)  
574 119–166. doi:<https://doi.org/10.3970/cmcs.2009.047.119>.
- 575 [34] Y. Liu, X. Wang, L. Wang, Z. Lv, A bayesian collocation method for static analysis of structures with unknown-but-  
576 bounded uncertainties, *Computer Methods in Applied Mechanics and Engineering* 346 (2019) 727–745. doi:<https://doi.org/10.1016/j.cma.2018.08.043>.
- 577
- 578 [35] H.-P. Wan, Y.-Q. Ni, A new approach for interval dynamic analysis of train-bridge system based on bayesian optimization,  
579 *Journal of Engineering Mechanics* 146 (5) (2020) 04020029. doi:[https://doi.org/10.1061/\(ASCE\)EM.1943-7889.0001735](https://doi.org/10.1061/(ASCE)EM.1943-7889.0001735).
- 580 [36] A. Ciciello, F. Giunta, Machine learning based optimization for interval uncertainty propagation, *Mechanical Systems*  
581 *and Signal Processing* 170 (2022) 108619. doi:<https://doi.org/10.1016/j.ymsp.2021.108619>.
- 582 [37] Z. Deng, Z. Guo, Interval identification of structural parameters using interval overlap ratio and monte carlo simulation,  
583 *Advances in Engineering Software* 121 (2018) 120–130.
- 584 [38] M. Imholz, M. Faes, D. Vandepitte, D. Moens, Robust uncertainty quantification in structural dynamics under scarce



- 585 experimental modal data: A bayesian-interval approach, *Journal of Sound and Vibration* 467 (2020) 114983.
- 586 [39] C. Jiang, Z. Zhang, Q. Zhang, X. Han, H. Xie, J. Liu, A new nonlinear interval programming method for uncertain  
587 problems with dependent interval variables, *European Journal of Operational Research* 238 (1) (2014) 245–253.
- 588 [40] C. K. Williams, C. E. Rasmussen, *Gaussian processes for machine learning*, Vol. 2, MIT press Cambridge, MA, 2006.
- 589 [41] D. Zhan, J. Qian, Y. Cheng, Pseudo expected improvement criterion for parallel EGO algorithm, *Journal of Global*  
590 *Optimization* 68 (3) (2017) 641–662. doi:<https://doi.org/10.1007/s10898-016-0484-7>.
- 591 [42] R. V. Rao, V. J. Savsani, D. Vakharia, Teaching–learning-based optimization: a novel method for constrained mechanical  
592 design optimization problems, *Computer-Aided Design* 43 (3) (2011) 303–315. doi:[https://doi.org/10.1016/j.cad.](https://doi.org/10.1016/j.cad.2010.12.015)  
593 [2010.12.015](https://doi.org/10.1016/j.cad.2010.12.015).
- 594 [43] A. S. Di Perrotolo, A theoretical framework for bayesian optimization convergence, Master’s thesis, KTH Royal Institute  
595 of Technology (2018).
- 596 [44] M. Schonlau, *Computer experiments and global optimization*, Ph.D. thesis, University of Waterloo (1997).
- 597 [45] D. Ginsbourger, R. L. Riche, L. Carraro, Kriging is well-suited to parallelize optimization, in: *Computational intelligence*  
598 *in expensive optimization problems*, Springer, 2010, pp. 131–162.
- 599 [46] C. Chevalier, D. Ginsbourger, Fast computation of the multi-points expected improvement with applications in batch  
600 selection, in: *International Conference on Learning and Intelligent Optimization*, Springer, 2013, pp. 59–69.
- 601 [47] A. Sóbester, S. J. Leary, A. J. Keane, A parallel updating scheme for approximating and optimizing high fidelity computer  
602 simulations, *Structural and multidisciplinary optimization* 27 (5) (2004) 371–383.
- 603 [48] D. Zhan, J. Qian, Y. Cheng, Balancing global and local search in parallel efficient global optimization algorithms, *Journal*  
604 *of Global Optimization* 67 (4) (2017) 873–892.
- 605 [49] F. A. Viana, R. T. Haftka, L. T. Watson, Efficient global optimization algorithm assisted by multiple surrogate techniques,  
606 *Journal of Global Optimization* 56 (2) (2013) 669–689.
- 607 [50] J. C. García-García, R. García-Ródenas, E. Codina, A surrogate-based cooperative optimization framework for computa-  
608 tionally expensive black-box problems, *Optimization and Engineering* 21 (3) (2020) 1053–1093.
- 609 [51] MATLAB and Global Optimization Toolbox Release 2018a, The MathWorks Inc., Natick, Massachusetts, United States,  
610 2018.
- 611 [52] Q. Gu, M. Barbato, J. P. Conte, P. E. Gill, F. McKenna, OpenSees-SNOPT framework for finite-element-based opti-  
612 mization of structural and geotechnical systems, *Journal of Structural Engineering* 138 (6) (2012) 822–834. doi:[https:](https://doi.org/10.1061/(ASCE)ST.1943-541X.0000511)  
613 [//doi.org/10.1061/\(ASCE\)ST.1943-541X.0000511](https://doi.org/10.1061/(ASCE)ST.1943-541X.0000511).